Published in final edited form as:
Nanomedicine (Lond). 2012 September ; 7(9): 1297–1309. doi:10.2217/nnm.12.14.

Prostate-targeted biodegradable nanoparticles loaded with androgen receptor silencing constructs eradicate xenograft tumors in mice

Jun Yang[1,2], **Sheng-Xue Xie**[3], **Yiling Huang**[1,4], **Min Ling**[1], **Jihong Liu**[2], **Yali Ran**[1], **Yanlin Wang**[4], **J Brantley Thrasher**[1], **Cory Berkland**[3], and **Benyi Li**[*,1,4]

[1]Department of Urology, The University of Kansas Medical Center, Kansas City, KS 66160, USA

[2]Department of Urology, Tongji Hospital, Huazhong University of Science & Technology, Wuhan 430030, China

[3]Departments of Pharmaceutical Chemistry & Chemical & Petroleum, Engineering, The University of Kansas, Lawrence, KS 66045, USA

[4]Departments of Pathology & Pharmacology, Three George, University School of Medicine, Yichang, 443000, China

Abstract

Background—Prostate cancer is the major cause of cancer death in men and the androgen receptor (AR) has been shown to play a critical role in the progression of the disease. Our previous reports showed that knocking down the expression of the *AR* gene using a siRNA-based approach in prostate cancer cells led to apoptotic cell death and xenograft tumor eradication. In this study, we utilized a biodegradable nanoparticle to deliver the therapeutic AR shRNA construct specifically to prostate cancer cells.

Materials & methods—The biodegradable nanoparticles were fabricated using a poly(DL-lactic-*co*-glycolic acid) polymer and the AR shRNA constructs were loaded inside the particles. The surface of the nanoparticles were then conjugated with prostate-specific membrane antigen aptamer A10 for prostate cancer cell-specific targeting.

Results—A10-conjugation largely enhanced cellular uptake of nanoparticles in both cell culture- and xenograft-based models. The efficacy of AR shRNA encapsulated in nanoparticles on *AR* gene silencing was confirmed in PC-3/AR-derived xenografts in nude mice. The therapeutic property of A10-conjugated AR shRNA-loaded nanoparticles was evaluated in xenograft models with different prostate cancer cell lines: 22RV1, LAPC-4 and LNCaP. Upon two injections of the AR shRNA-loaded nanoparticles, rapid tumor regression was observed over 2 weeks. Consistent with previous reports, A10 aptamer conjugation significantly enhanced xenograft tumor regression compared with nonconjugated nanoparticles.

[*]Author for correspondence: Tel.: +1 913 588 4773, bli@kumc.edu.

Financial & competing interests disclosure
The authors have no other relevant affiliations or financial involvement with any organization or entity with a financial interest in or financial conflict with the subject matter or materials discussed in the manuscript apart from those disclosed.
No writing assistance was utilized in the production of this manuscript.

Ethical conduct of research
The authors state that they have obtained appropriate institutional review board approval or have followed the principles outlined in the Declaration of Helsinki for all human or animal experimental investigations. In addition, for investigations involving human subjects, informed consent has been obtained from the participants involved.

Discussion—These data demonstrated that tissue-specific delivery of AR shRNA using a biodegradable nanoparticle approach represents a novel therapy for life-threatening prostate cancers.

Keywords

androgen receptor; aptamer; nanoparticle; prostate cancer; prostate-specific membrane antigen; siRNA

Prostate cancer is one of the major causes of cancer death among men in the USA [1]. Medical treatment for metastatic prostate cancer has relied heavily on androgen ablation. Unfortunately, most patients treated by androgen ablation ultimately relapse to more aggressive castration-resistant cancers [2]. The etiology of castration-resistant progression of prostate cancers may have various molecular causes, but in most cases, androgen receptor (AR) expression is maintained [3,4]. Recent studies have demonstrated that AR signaling is required for prostate cancer progression [5–10]. Consistently, we and others have shown that suppression of *AR* gene expression by siRNA-mediated *AR* gene silencing led to reduced tumor growth in AR-positive prostate cancers [11–15]. Therefore, this AR siRNA-based approach provides a powerful gene therapy for advanced prostate cancers.

Successful delivery of therapeutic agents efficiently and specifically to the target tissue/cell is desirable for the treatment of human cancers. A current drug delivery hotspot is polymeric nanoparticles (NPs), which do not have the side effects of traditional viral vectors (i.e., insertional mutagenesis and immunogenesis) or liposome vehicles (i.e., toxicity and inefficiency). Properly designed NPs can be delivered specifically to a target tissue and the encapsulated drug can then be released inside the targeted cells after degradation of the NP matrix without affecting surrounding tissues [16,17]. Nanoparticles that have a hydrophilic surface can avoid uptake by the reticuloendothelial system and passively accumulate in tumors due to the enhanced permeability and retention effect in leaky tumor vasculature [17,18]. Additional coatings (i.e., polyethylene glycol [PEG]) can further increase their circulating time by repelling plasma proteins [18].

The prostate-specific membrane antigen (PSMA) is a well-known tumor antigen and it is primarily expressed on the surface of prostate cancer epithelial cells and also has been reported to be expressed on the tumor microvasculature and other organs and tissues [19,20]. This cell surface expression pattern and its elevated levels in metastatic prostate cancers warranted it as a promising target for the diagnosis, detection and management of prostate cancer [20]. As such, PSMA has currently been used for molecular imaging, cancer vaccine development and targeted drug delivery in prostate cancers. In particular, a RNA-based aptamer targeting human PSMA was developed (PSMA-A10), which interacts specifically with the PSMA extracellular domain [21].

In order to maintain sustained gene silencing in cells, a common approach is to stably transfect the cells with a hairpin-structured siRNA under the control of a promoter, such as CMV, U6 or H1 RNA polymerase promoter [22]. Thus, we designed a hairpin structure based on AR siRNA sequences and then generated an adeno-associated virus (AAV) that bears the hairpin-structured AR siRNA (ARHP8) sequence [7,23]. Local or systemic delivery of the AAV-ARHP8 virus to nude mice bearing human prostate cancer xenografts abolished tumor growth regardless of their hormone responsiveness [13]. These previous studies provide strong support for the therapeutic property of the AR siRNA-based strategy.

As a delivery vehicle for targeted therapy, NPs could be functionalized to have high tissue/cell selectivity to avoid systemic side effects and long bloodstream circulating time to

increase the efficiency of the delivered therapeutic agents. Over other polymers, biodegradable poly-$_{DL}$-lactic-*co*-glycolic acid (PLGA) offers advantages of being fully biodegradable *in vivo* and has been approved for use in humans by the US FDA [24]. PSMA aptamer-mediated prostate cancer cell-specific targeting has been demonstrated recently [25–34]. Therefore, we developed a strategy using PSMA aptamer-conjugated PLGA NPs to deliver the AR shRNA constructs for AR silencing. Our results demonstrated that this strategy successfully delivered the AR shRNA constructs specifically into prostate cancer cells, resulting in effective tumor eradication *in vivo*.

Materials & methods

Fabrication of PLGA-PEG-COOH NPs encapsulating the plasmid DNA

PLGA (50:50; inherent viscosity: 0.67 dl/g; molecular weight ~100 kDa) was purchased from Absorbable Polymers (AL, USA). 2, 2, 2-trifluoro-ethanol was purchased from ACROS (NJ, USA). Pluronic® F127 was purchased from Sigma-Aldrich (MO, USA). Plasmid DNAs (pAAV-green fluorescent protein [GFP] and pAAVA-RHP8-GFP) were purified using QIAGEN Giga kits. AR siRNA targeting sequence (5′-AAGAAGGC CAGUUGUAUGGAC-3′) and AR shRNA construction (5′-GAAGGCCAGTTGTATG GACttcaagagaGTCCATACAACTGGCCTTC-3′) were described in our previous reports [7,23].

PLGA NPs were prepared by a solvent diffusion method. Briefly, 0.8 ml of 18 mg/ml PLGA solution dissolved in 2, 2, 2-trifluoroethanol was mixed with 0.2 ml of DNA solution containing 200–500 μg DNA dissolved in TE buffer (pH 8.0). The mixture was added to 10 ml 0.1% modified Pluronic® F127-COOH (the hydroxyl groups of Pluronic® F127 were changed to carboxyl groups) through a syringe pump (17.5 ml/h) under stirring at 250 rpm. The modified Pluronic® F127 was utilized as a surfactant to impart reactive carboxyl groups on the particle surface. The NPs that were produced were dialyzed using a 1000 kDa molecular weight cutoff membrane for 12–16 h, refreshing the dialysate twice.

Characterization of the size & surface charge of PLGA NPs

The sizes and zeta potentials of the PLGA NPs were determined using a ZetaPALS dynamic light scattering system (ZetaPALS, Brookhaven Instruments Corp., NY, USA).

Conjugation of aptamer to PLGA NPs

A suspension of Pluronic® F127-COOH-coated PLGA NPs was buffered using 2-(*N*-morpholino) ethanesulfonic acid, pH 6.5. Nanoparticles were then incubated with 100 mM 1-ethyl-3-(3-dimethylaminopropyl) carbodiimide hydrochloride and 50 mM *N*-hydroxysulfosuccinimide for 15 min. The activated carboxyl terminus of Pluronic® F127-COOH on the surface of NPs was allowed to react with the amino terminus of the aptamer (15 mM) for at least 6 h at room temperature. Conjugated NPs were dialyzed with purified water. Size and charge of NP and aptamer-NP were characterized using dynamic light scattering (ZetaPALS). The amount of free aptamer after the reaction was quantified by reverse phase HPLC on a Vydac® Protein and Peptide C18 column with a gradient of 5–90% acetonitrile over 30 min. The peaks were monitored by UV absorbance at 260 nm. The density of aptamer on the surface of NPs was calculated from the total surface area assuming a normal Guassian particle size distribution.

Determination of the plasmid DNA/aptamer entrapment efficiency & release from PLGA–PEG NP formulations *in vitro*

Briefly, 500 μl of various NP suspensions was centrifuged. The pellet was washed three-times using 1.5 ml water. Then, 500 μl chloroform was added to dissolve the pellet and 1 ml

TE buffer (pH 8.0) was added to extract DNA from the organic phase. After centrifugation, the UV absorbance at 260 nm was used to quantify DNA in the TE buffer phase (Table 1). DNA/aptamer extraction was also visualized on a 1% agarose gel after ethidium bromide staining.

Cell culture & cellular uptake of NPs *in vitro*

Human prostate cancer cell lines LAPC-4, LNCaP, 22RV1 and PC-3/AR were grown in the conditions as described previously [7,13]. For assessing cellular uptake of NPs, cells were plated in 12-well plates overnight and the suspension of NPs was added to the culture. At designated time-points, cell nuclei DNA was stained with nuclear dye Hoechst 33324 for 5 min. The percentage of cells that displayed positive fluorescence were quantitatively counted from five to ten microscopic fields and the representative micrographs were acquired using a fluorescent microscope (Olympus, Japan).

RNA extraction, reverse transcription-PCR & western blot assays

Total RNA was extracted using TriZol™ reagent (Invitrogen, CA, USA) from cultured cells, xenograft tissues and mouse organs. Reverse transcription (RT)-PCR was carried out using a RETROscript™ kit (Ambion, TX, USA) to assess *AR* gene expression at the mRNA level. The primers for the AR and S18 ribosome RNA were described in our recent publications [7,13]. For quantitative PCR, a different pair of AR primers (forward: 5′-GAAAGCGACTTCACCGCACCTG-3′; backward 5′-ACATGGTCCCTGGCAGTCTCC-3′) was used. S18 primers was used as internal control.

For western blot analysis, protein samples were extracted from cell lysates or xenograft tumors that were snap-frozen and stored at 80°C. Equal amounts of protein were subjected to SDS-PAGE and then western blot for assessing AR expression. Actin blot served as a protein-loading control. Antibodies for AR (clone 441) and actin were purchased from Santa Cruz Biotechnology (CA, USA).

Animal xenograft model, DNA extraction & quantitative PCR

Athymic NCr-nu/nu male mice (NCI-Frederick, Fort Detrick, VA, USA) were maintained in accordance with the Institutional Animal Care and Use Committee procedures and guidelines. Xenograft tumors were established as described in our recent publication [13,39]. Briefly, exponentially grown cells were trypsinized and resuspended in phosphate-buffered saline. A total of 2.0×10^6 cells was resuspended in RPMI-1640/10% fetal bovine serum with a 4:1 v/v ratio of Matrigel™ (BD Bioscience, MA, USA), and was injected subcutaneously into the rear flanks or the dosal-lateral loops of the prostate. For subcutaneous xenografts, when tumors were palpable (30–50 mm^3 in 4–6 weeks), animals were divided into different groups for treatment with NPs. As described in the legends of Figures 1 & 2, NPs were injected systemically via tail vein. Tumor growth was monitored by measuring the length (L) and the width (W), and the volume was calculated using Equation 1:

$$V=(L \times W^2)/2 \quad (1)$$

For orthotropic xenograft models, blood samples were collected by tail incision and serum prostate-specific antigen (PSA) levels were determined using a commercial ELISA kit (Abnova, CA, USA). At necropsy, prostate loops were harvested and their wet weights were recorded before snap-frozen.

Statistical analysis

Western blot, fluorescent images and RT-PCR results were presented from a representative experiment. The mean and standard error of the mean from cell counting and animal experiments are shown. The differences between treatment and control groups were analyzed using the SPSS software (SPSS, IL, USA).

Results

Preparation & characterization of plasmid DNA-loaded aptamer-conjugated PLGA NPs

Polymeric particles serve as a common carrier and controlled release delivery system for DNA [24]. Many particle formation processes utilize harsh homogenization or ultrasonication to disperse a solution of the polymer phase into an aqueous phase where solvent extraction from the polymer phase takes place. The shear associated with these processing conditions requires intensification to create increasingly smaller particle sizes, often damaging plasmid DNA to linear or fragmented forms [35]. In this study, we utilized a solvent diffusion technique that reduced shear and improved retention of DNA structure [36–38]. Phenol/chloroform extraction assay revealed that PSMA aptamers were successfully conjugated onto the surface of the PLGA NPs (Figure 3B).

Aptamer conjugation enhances AR shRNA-mediated gene silencing & cell death

As reported in our previous publication, AR silencing led to profound apoptotic cell death in AR-native prostate cancer cells, and systemic delivery of the AR silencing viral particles eradicated prostate cancer xenografts in nude mice [7,13]. Due to the safety concern of viral vectors for clinical use, we developed a strategy that utilizes the PLGA-based NP to deliver the AR shRNA construct.

First, we evaluated cellular uptake of the NPs with or without A10 aptamer. Nile-red fluorescent dye was encapsulated into the NPs as an indicator of cellular uptake. PSMA-positive human prostate cancer LNCaP cells were used for the testing. As shown in Figure 4, A10 aptamer-conjugated NPs bound to cells more rapidly than the nonaptamer-conjugated NPs in a dose- and time-dependent manner.

Next, we evaluated the cellular uptake *in vivo* using a mouse xenograft model derived from human prostate cancer 22RV1 cells. As shown in Figure 4D, A10 aptamer-conjugated NPs were uptaken by 22RV1 xenografts much faster and to a greater extent than nonaptamer-conjugated NPs. These data are supported by previous reports showing that PSMA aptamer conjugation exhibits strong, differential delivery to prostate cancer cells [25–34].

To determine the efficacy of A10 aptamer-conjugated NPs on plasmid DNA delivery for *AR* gene silencing, we then used the A10-NPs to deliver ARHP8 constructs. We first tested A10-NP-mediated *AR* gene silencing in LNCaP cells. A10-conjugated or naked (no A10 conjugation) NPs loaded with ARHP8 constructs were added into cell culture. Cells were harvested 5 days later and total RNAs were extracted for RT-PCR assay. As shown in Figure 5A, naked or A10-conjugated NPs loaded with GFP-expressing constructs had no effect on *AR* gene expression. By contrast, ARHP8 construct-loaded NPs induced a significant reduction of *AR* gene expression at the mRNA and protein levels compared with the control, of which A10 conjugation dramatically enhanced the AR silencing effect. Similar results were also obtained in LAPC-4 (Figure 5B). Quantitative RT-PCR also revealed that A10 conjugation significantly enhanced ARHP8-induced *AR* gene silencing (Figure 5C). These data indicated that the strategy using A10 PSMA aptamer-conjugated NPs largely increases NP uptake, and the A10-conjugated PLGA NP is capable of delivering AR shRNA plasmid vector for gene silencing.

Aptamer-conjugated AR shRNA-loaded NPs eradicated xenograft tumors

Before testing the antitumor effect of NP-encapsulated ARHP8 shRNA in a large group setting, we first performed a pilot animal study to determine the minimum dose of NPs for efficient *AR* gene silencing in the xenograft tumors after intravenous injection. Mouse subcutaneous xenograft tumors were established with PC-3/AR cells, which were described in our previous publication [7]. Because PC-3 cells are PSMA negative, we used naked NPs to deliver the ARHP8 plasmid. Meanwhile, since cell survival for PC-3 cells is not dependent on *AR* gene expression, knocking down AR expression will not affect xenograft tumor growth derived from PC-3 cells. When the tumor is palpable (~50 mm^3 in 4–6 weeks), five different doses of NPs that contain 1.0, 2.0, 4.0, 6.0 or 8.0 μg ARHP8 plasmid DNA were injected via tail vein into the animals. In addition, one animal received phosphate-buffered saline as negative control. The tumors and other organs (liver, spleen, kidney, testes, intestine and lung) were harvested 1 week later. Total RNA extracts from the tumor samples were used to evaluate AR mRNA levels and protein extracts from tumor tissues were used to assess AR protein expression by immunoblotting. As shown in Figures 6A & 6B, a dose-dependent reduction of AR expression at the mRNA and protein levels was noticed and the effective dose for AR silencing was ≥4.0 μg plasmid DNA-loaded NPs, which was then used in the following experiments. Tissue distribution of the NPs was analyzed by PCR reactions for GFP sequence with the genomic DNA samples extracted from xenograft tumors and various organs (Figure 6C), and the analysis revealed that most of the NPs were retained in xenograft tumors, followed by prostate, liver, spleen, kidney and testis. Since PC-3/AR cells are not dependent on functional AR to survive, injection of ARHP8 NPs had no effect on tumor growth.

We next investigated the antitumor effect of the A10-conjugated ARHP8-encapsulated NPs in a large group of xenograft-bearing nude mice. We used three cell lines, castration-resistant 22RV1 cells, and androgen-responsive LAPC-4 and LNCaP to generate xenografts in nude mice as described in our previous publication [39]. Once the tumors were palpable (~30–50 mm^3), animals received two tail vein injections of NPs with an interval of 1 week (Figure 1). Tumor growth was monitored three-times a week. Due to the heavy burden of xenograft tumors in the control groups, animals were sacrificed at day 21 (3 weeks) after the first treatment. As shown in Figure 1A, injection of ARHP8-encapsulated NPs (Nano-ARHP8) significantly reduced the tumor growth of 22RV1 xenografts compared with the control NPs (Nano-GFP). In Nano-ARHP8-treated animals, xenograft tumors eventually disappeared, which is similar to our previous finding when ARHP8 shRNA was delivered with AAV approach [13]. Most importantly, however, treatment with A10-conjugated ARHP8 NPs led to an even more rapid tumor eradication compared with the treatment with naked ARHP8 NPs (14 days in A10-conjugated PLGA vs 17 days in naked PLGA). These data are consistent with previous reports that PSMA aptamer conjugation enhances PLGA NP-mediated ARHP8 transfection in prostate cancer cells [25–27].

Since the pioneer work from other groups demonstrated the efficacy of PSMA aptamer (A10)-mediated prostate cancer cell targeting [29–32], we did not include naked PLGA NP groups in our next animal studies but instead focused on the comparison of ARHP8-loaded versus GFP-loaded A10-PLGA NPs. As seen in Figures 1B & 1C, in comparison with the control GFP construct-loaded A10-PLGA NPs, treatment with ARHP8-loaded A10-PLGA NPs led to a rapid regression of xenograft tumors derived from LAPC4 or LNCaP cells. These data indicated that PLGA NPs represent a feasible approach to replace the AAV strategy for ARHP8 construct delivery for *in vivo* AR silencing.

In addition, we tested the antitumor effect of Nano-ARHP8 with or without the PSMA aptamer A10 conjugation in orthotopic xenograft model. LNCaP cells were inoculated in nude mouse prostate (dorsal-lateral loops). Mouse serum levels of human PSA were

monitored as a sign for tumor development. After 4 weeks, once the mouse serum PSA reached 70–90 ng/ml, animals were divided into three groups and received different treatments. As shown in Figure 2, serum PSA levels steadily increased in the control group that received GFP NPs, representing a typical pattern of tumor growth *in vivo*. Conversely, treatment with ARHP8-loaded PLGA NPs resulted in a dramatic decrease in serum PSA level, indicating a rapid tumor regression. In comparison, treatment with A10-Nano-ARHP8 further enhanced the rapid decrease in serum PSA levels.

At the end of experiments, animals were sacrificed, the prostate loops together with seminal vesicles were dissected and their wet weights were recorded. In groups that received either A10-Nano-ARHP8 or naked ARHP8 NPs, prostate wet weight was significantly lower than that in A10-Nano-GFP-treated animals (Figure 2B), suggesting that ARHP8 NPs reduced tumor growth. RT-PCR analysis revealed that treatment with A10-Nano-ARHP8 NPs dramatically reduced *AR* gene expression compared with the control group, although Nano-ARHP8 also moderately reduced *AR* gene level (Figure 2C). These data were supported by the results from *in vitro* cell culture-based experiments (Figure 5) and our previous animal studies with AAV approach [13], indicating that PLGA NPs loaded with ARHP8 constructs induced *AR* gene silencing and that A10 conjugation enhanced the effect of ARHP8-loaded PLGA NPs on *AR* gene silencing *in vivo*.

Finally, we analyzed the copy numbers of ARHP8 constructs in xenograft tumor tissues. Genomic DNA samples were extracted from tumor tissues of LNCaP and 22RV1 xenografts obtained from the subcutaneous xenograft models (Figures 1A & 1C). Quantitative PCR assays were conducted to assess the DNA content of GFP sequence derived from the plasmid construct. Serially diluted samples of GFP-ARHP8 construct were used to generate the quantitative PCR standard curve. As shown in Figure 7A, a linear curve was obtained by plotting the quantitative PCR results with the concentrations of GFP-ARHP8 plasmid constructs. Consistent with the antitumor effect, in both LNCaP and 22RV1 xenografts, A10-conjugated NPs yielded a much higher DNA content in xenograft tumors than nonconjugated NPs (Figure 7B). Together with other results from Figures 1A, 2A, 4 & 5, our study clearly confirmed the notion that PSMA A10 conjugation enhances PLGA NP retention in prostate cancer cells compared with the naked ones.

Discussion

In this study, we continued our previous work of AR siRNA-based gene therapy for prostate cancers [7,13]. The biodegradable PLGA polymer-based NPs were utilized to deliver the AR shRNA constructs and prostate cancer-specific targeting was achieved by conjugating the NP surface with PSMA A10 aptamers. Our cell culture- and xenograft-based testing revealed that PLGA-mediated delivery of AR shRNA constructs yielded an effective *AR* gene silencing and A10 conjugation largely enhanced the antitumor effect of AR shRNA NPs. These results strongly suggest that the A10-conjugated ARHP8 construct-loaded PLGA NP represents a novel gene therapy for prostate cancers.

Recently, PLGA NPs were widely used for drug delivery studies [40–42]. Our previous work illustrated the advantages of monodisperse particles in controlling the release kinetics of drugs from the polymer matrix [36–38]. Our recent studies also indicated that particle size can be optimized for different delivery purposes and plasmid DNA constructs can be encapsulated without any damage [43]. In this study, our data further confirmed that the solvent diffusion method for PLGA NP fabrication retained DNA function.

The RNA aptamer A10 is a ligand for PSMA and was widely used to achieve prostate-specific targeting [21]. The A10 aptamer has been used to conjugate with various NPs for

targeted chemotherapy [25–30] and molecular imaging [31,32], or to form chimeras with shRNA constructs for targeted gene therapy [33,34]. In this study, we used a PEG-spacer (the hydrophilic blocks of Pluronic F127) to conjugate the A10 onto the NPs. The carboxylic acid end group of modified Pluronic F127-COOH on the surface of PLGA NPs was conjugated to an amine-modified version of the A10 aptamer. The purpose of the PEG spacer was to avoid absorption of blood proteins and extend NP circulation.

The key component of the NP is the AR silencing construct, which is a plasmid vector that bears a hairpin-structured siRNA sequence against the human *AR* gene. This construct, pU6-ARHP8-hGFP, were used to generate AAV particles that was previously proven to effectively silence the *AR* gene in prostate cancer cells [7] and xenograft tumor regression in mice [13]. This construct carries a secondary coding sequence for humanized GFP protein linked by a polivirus IRES sequence after the ARHP8 cassette, providing the extra feature of a GFP marker for monitoring tissue distribution of the NPs. Our results with the Nano-ARHP8 approach in this study were comparable to our previously reported AAV approach [13], leading to xenograft regression within 2 weeks of treatment. However, PLGA NPs have multiple advantages over viral vectors, such as biodegradability, surface conjugation of targeting moieties, possible loading of multiple components, the possibility of limited toxicity or immunogenicity. In addition, A10 conjugation provided superb efficacy over the naked NP, as evidenced by a quicker recession of xenograft tumors.

In conclusion, we developed a novel strategy of PSMA-targeted NPs loaded with AR shRNA constructs for prostate cancer gene therapy. The NPs were fabricated with biodegradable PLGA polymers, whose surfaces were conjugated with PSMA aptamer A10 as the targeting moiety. Our *in vitro* and *in vivo* testing demonstrated that ARHP8-loaded PLGA NPs mediated *AR* gene silencing *in vitro* and *in vivo*, and that A10 conjugation enhanced cellular uptake of ARHP8-loaded NPs. Upon systemic delivery of the ARHP8-loaded NPs, rapid PSA decline and tumor regression were observed in 2 weeks. In addition, A10 conjugation enhanced PSA decline and xenograft tumor regression compared with nonconjugated NPs. Prostate-specific delivery of ARHP8 shRNA constructs using biodegradable NPs represents a novel therapy for prostate cancers with efficacy rivaling our prior studies employing viral vectors.

Acknowledgments

We thank the staff in KUMC LAR for excellent assistance in animal care. This study was supported by Department of Defense Idea Development Awards (W81XWH-04-1-0214 and W81XWH-07-1-0021). This work was also partially supported by KU William L Valk Endowment and Kansas Masonic Foundation through KU Cancer Center pilot grant to Benyi Li. C Berkland would like to acknowledge supports for the project from the Coulter Foundation, the NIH (AR054035) and the NSF (0966614).

References

Papers of special note have been highlighted as:

- ■ of interest
- ■■ of considerable interest

1. Jemal A, Siegel R, Xu J, Ward E. Cancer statistics, 2010. CA Cancer J. Clin. 2010; 60(5):277–300. [PubMed: 20610543]
2. Scher HI, Sawyers CL. Biology of progressive, castration-resistant prostate cancer: directed therapies targeting the androgen-receptor signaling axis. J. Clin. Oncol. 2005; 23:8253–8261. [PubMed: 16278481]

3. Shen MM, Abate-Shen C. Molecular genetics of prostate cancer: new prospects for old challenges. Genes Dev. 2010; 24(18):1967–2000. [PubMed: 20844012]
4. Li B, Thrasher JB. Androgen receptor and cellular survival in prostate cancer. Rec. Res. Dev. Cancer. 2005; 7:65–89.
5. Chen CD, Welsbie DS, Tran C, et al. Molecular determinants of resistance to antiandrogen therapy. Nat. Med. 2004; 10(1):33–39. [PubMed: 14702632] ■■ Comprehensive study showing the critical role of androgen receptor (AR) in prostate cancer progression.
6. Stanbrough M, Leav I, Kwan PW, Bubley GJ, Balk SP. Prostatic intraepithelial neoplasia in mice expressing an androgen receptor transgene in prostate epithelium. Proc. Natl Acad. Sci. USA. 2001; 98(19):10823–10828. [PubMed: 11535819]
7. Liao X, Tang S, Thrasher JB, Griebling TL, Li B. Small-interfering RNA-induced androgen receptor silencing leads to apoptotic cell death in prostate cancer. Mol. Cancer Ther. 2005; 4(4): 505–515. [PubMed: 15827323] ■■ The first report showing AR siRNA-induced cell death in prostate cancer cells.
8. Zegarra-Moro OL, Schmidt LJ, Huang H, Tindall DJ. Disruption of androgen receptor function inhibits proliferation of androgen-refractory prostate cancer cells. Cancer Res. 2002; 62(4):1008–1013. [PubMed: 11861374] ■ A study demonstrating the functional role of AR for prostate cancer survival and proliferation with blocking anti-AR antibodies.
9. Zhang L, Johnson M, Le KH, et al. Interrogating androgen receptor function in recurrent prostate cancer. Cancer Res. 2003; 63(15):4552–4560. [PubMed: 12907631]
10. Li TH, Zhao H, Peng Y, Beliakoff J, Brooks JD, Sun Z. A promoting role of androgen receptor in androgen-sensitive and -insensitive prostate cancer cells. Nucleic Acids Res. 2007; 35:2767–2776. [PubMed: 17426117]
11. Snoek R, Cheng H, Margiotti K, et al. *In vivo* knockdown of the androgen receptor results in growth inhibition and regression of well-established, castration-resistant prostate tumors. Clin. Cancer Res. 2009; 15(1):39–47. [PubMed: 19118031]
12. Cheng H, Snoek R, Ghaidi F, Cox ME, Rennie PS. Short hairpin RNA knockdown of the androgen receptor attenuates ligand-independent activation and delays tumor progression. Cancer Res. 2006; 66(21):10613–10620. [PubMed: 17079486]
13. Sun A, Tang J, Terranova PF, Zhang X, Thrasher JB, Li B. Adeno-associated virus-delivered short hairpin-structured RNA for androgen receptor gene silencing induces tumor eradication of prostate cancer xenografts in nude mice: a preclinical study. Int. J. Cancer. 2010; 126(3):764–774. [PubMed: 19642108] ■■ Adeno-associated virus-based systemic delivery of AR shRNA constructs for AR silencing and tumor eradication.
14. Compagno D, Merle C, Morin A, et al. SIRNA-directed *in vivo* silencing of androgen receptor inhibits the growth of castration-resistant prostate carcinomas. PLoS ONE. 2007; 2(10):e1006. [PubMed: 17925854] ■ Intraperitoneal delivery of naked siRNA molecules for AR silencing and tumor suppression.
15. Azuma K, Nakashiro K, Sasaki T, et al. Antitumor effect of small interfering RNA targeting the androgen receptor in human androgen-independent prostate cancer cells. Biochem. Biophys. Res. Commun. 2010; 391(1):1075–1079. [PubMed: 20004643]
16. Brannon-Peppas L, Blanchette JO. Nanoparticle and targeted systems for cancer therapy. Adv. Drug Deliv. Rev. 2004; 56(11):1649–1659. [PubMed: 15350294]
17. Jain RK, Stylianopoulos T. Delivering nanomedicine to solid tumors. Nat. Rev. Clin. Oncol. 2010; 7(11):653–664. [PubMed: 20838415]
18. Sengupta S, Eavarone D, Capila I, et al. Temporal targeting of tumour cells and neovasculature with a nanoscale delivery system. Nature. 2005; 436(7050):568–572. [PubMed: 16049491]
19. Wright GL Jr, Haley C, Beckett ML, Schellhammer PF. Expression of prostate-specific membrane antigen in normal, benign, and malignant prostate tissues. Urol. Oncol. 1995; 1(1):18–28. [PubMed: 21224086]
20. Katsogiannou M, Peng L, Catapano CV, Rocchi P. Active-targeted nanotherapy strategies for prostate cancer. Curr. Cancer Drug Targets. 2011; 11(8):954–965. [PubMed: 21861840]
21. Lupold SE, Hicke BJ, Lin Y, Coffey DS. Identification and characterization of nuclease-stabilized RNA molecules that bind human prostate cancer cells via the prostate-specific membrane antigen.

Cancer Res. 2002; 62:4029–4033. [PubMed: 12124337] ■■ The first report of prostate-specific membrane antigen aptamer synthesis and evaluation.

22. Brummelkamp TR, Bernards R, Agami R. A system for stable expression of short interfering RNAs in mammalian cells. Science. 2002; 296:550–553. [PubMed: 11910072]
23. Shanmugam I, Cheng G, Terranova PF, Thrasher JB, Thomas CP, Li B. Serum/glucocorticoid-induced protein kinase-1 facilitates androgen receptor-dependent cell survival. Cell Death Differ. 2007; 14(12):2085–2094. [PubMed: 17932503]
24. Bala I, Hariharan S, Kumar MN. PLGA nanoparticles in drug delivery: the state of the art. Crit. Rev. Ther. Drug Carrier Syst. 2004; 21(5):387–422. [PubMed: 15719481]
25. Dhar S, Gu FX, Langer R, Farokhzad OC, Lippard SJ. Targeted delivery of cisplatin to prostate cancer cells by aptamer functionalized Pt(IV) prodrug-PLGA–PEG nanoparticles. Proc. Natl Acad. Sci. USA. 2008; 105(45):17356–17361. [PubMed: 18978032]
26. Farokhzad OC, Cheng J, Teply BA, et al. Targeted nanoparticle-aptamer bioconjugates for cancer chemotherapy *in vivo*. Proc. Natl Acad. Sci. USA. 2006; 103(16):6315–6320. [PubMed: 16606824] ■ A successful use of prostate-specific membrane antigen aptamer-conjugated poly-DL-lactic-*co*-glycolic acid nanoparticle for *in vivo* delivery of chemotherapy agents.
27. Cheng J, Teply BA, Sherifi I, et al. Formulation of functionalized PLGA–PEG nanoparticles for *in vivo* targeted drug delivery. Biomaterials. 2007; 28(5):869–876. [PubMed: 17055572]
28. Dhar S, Kolishetti N, Lippard SJ, Farokhzad OC. Targeted delivery of a cisplatin prodrug for safer and more effective prostate cancer therapy in vivo. Proc. Natl Acad. Sci. USA. 2011; 108(5): 1850–1855. [PubMed: 21233423]
29. Gu F, Zhang L, Teply BA, et al. Precise engineering of targeted nanoparticles by using self-assembled biointegrated block copolymers. Proc. Natl Acad. Sci. USA. 2008; 105(7):2586–2591. [PubMed: 18272481]
30. Sanna V, Roggio AM, Posadino AM, et al. Novel docetaxel-loaded nanoparticles based on poly(lactide-*co*-caprolactone) and poly(lactide-*co*-glycolide-*co*-caprolactone) for prostate cancer treatment: formulation, characterization, and cytotoxicity studies. Nanoscale Res. Lett. 2011; 6(1): 260. [PubMed: 21711774]
31. Kim D, Jeong YY, Jon S. A drug-loaded aptamer-gold nanoparticle bioconjugate for combined CT imaging and therapy of prostate cancer. ACS Nano. 2010; 4(7):3689–3696. [PubMed: 20550178]
32. Yu MK, Kim D, Lee IH, So JS, Jeong YY, Jon S. Image-guided prostate cancer therapy using aptamer-functionalized thermally cross-linked superparamagnetic iron oxide nanoparticles. Small. 2011; 7(15):2241–2249. [PubMed: 21648076]
33. Ni X, Zhang Y, Ribas J, et al. Prostate-targeted radiosensitization via aptamer-shRNA chimeras in human tumor xenografts. J. Clin Invest. 2011; 121(6):2383–2390. [PubMed: 21555850]
34. Dassie JP, Liu XY, Thomas GS, et al. Systemic administration of optimized aptamer-siRNA chimeras promotes regression of PSMA-expressing tumors. Nat. Biotechnol. 2009; 27(9):839–849. [PubMed: 19701187]
35. Li Y, Ogris M, Pelisek J, Röedl W. Stability and release characteristics of poly(d,l-lactide-*co*-glycolide) encapsulated CaPi-DNA coprecipitation. Int. J. Pharm. 2004; 269(1):61–70. [PubMed: 14698577]
36. Chittasupho C, Shannon L, Siahaan TJ, Vines CM, Berkland C. Nanoparticles targeting dendritic cell surface molecules effectively block T cell conjugation and shift response. ACS Nano. 2011; 5(3):1693–1702. [PubMed: 21375342]
37. Chittasupho C, Manikwar P, Krise JP, Siahaan TJ, Berkland C. cIBR effectively targets nanoparticles to LFA-1 on acute lymphoblastic T cells. Mol. Pharm. 2010; 7(1):146–155. [PubMed: 19883077]
38. Chittasupho C, Xie SX, Baoum A, Yakovleva T, Siahaan TJ, Berkland CJ. ICAM-1 targeting of doxorubicin-loaded PLGA nanoparticles to lung epithelial cells. Eur. J. Pharm Sci. 2009; 37(2): 141–150. [PubMed: 19429421]
39. Li B, Sun A, Youn H. Conditional Akt activation promotes androgen-independent progression of prostate cancer. Carcinogenesis. 2007; 28(3):572–583. [PubMed: 17032658]
40. Venier-Julienne MC, Benoît JP. Preparation, purification and morphology of polymeric nanoparticles as drug carriers. Pharm. Acta Helv. 1996; 71(2):121–128. [PubMed: 8810578] ■

Original publication for the invention of poly-DL-lactic-*co*-glycolic acid polymer-based nanoparticles.

41. Astete CE, Sabliov CM. Synthesis and characterization of PLGA nanoparticles. J. Biomater. Sci. Polym. Ed. 2006; 17(3):247–289. [PubMed: 16689015]
42. Mohamed F, van der Walle CF. Engineering biodegradable polyester particles with specific drug targeting and drug release properties. J. Pharm Sci. 2008; 97(1):71–87. [PubMed: 17722085]
43. Baoum A, Dhillon N, Buch S, Berkland C. Cationic surface modification of PLG nanoparticles offers sustained gene delivery to pulmonary epithelial cells. J. Pharm. Sci. 2010; 99(5):2413–2422. [PubMed: 19911425]

Executive summary

- Biodegradable poly-$_{DL}$-lactic-*co*-glycolic acid polymer-based nanoparticles can be used to encapsulate androgen receptor (AR) shRNA constructs.
- Surface conjugation of prostate-specific membrane antigen aptamer A10 enhanced cellular uptake of nanoparticles *in vitro* and *in vivo*.
- AR shRNA-loaded nanoparticles led to rapid tumor regression.
- Prostate-specific membrane antigen A10 mediated prostate-specific delivery of poly-$_{DL}$-lactic-*co*-glycolic acid nanoparticles loaded with AR shRNA represents a novel therapy for prostate cancers.

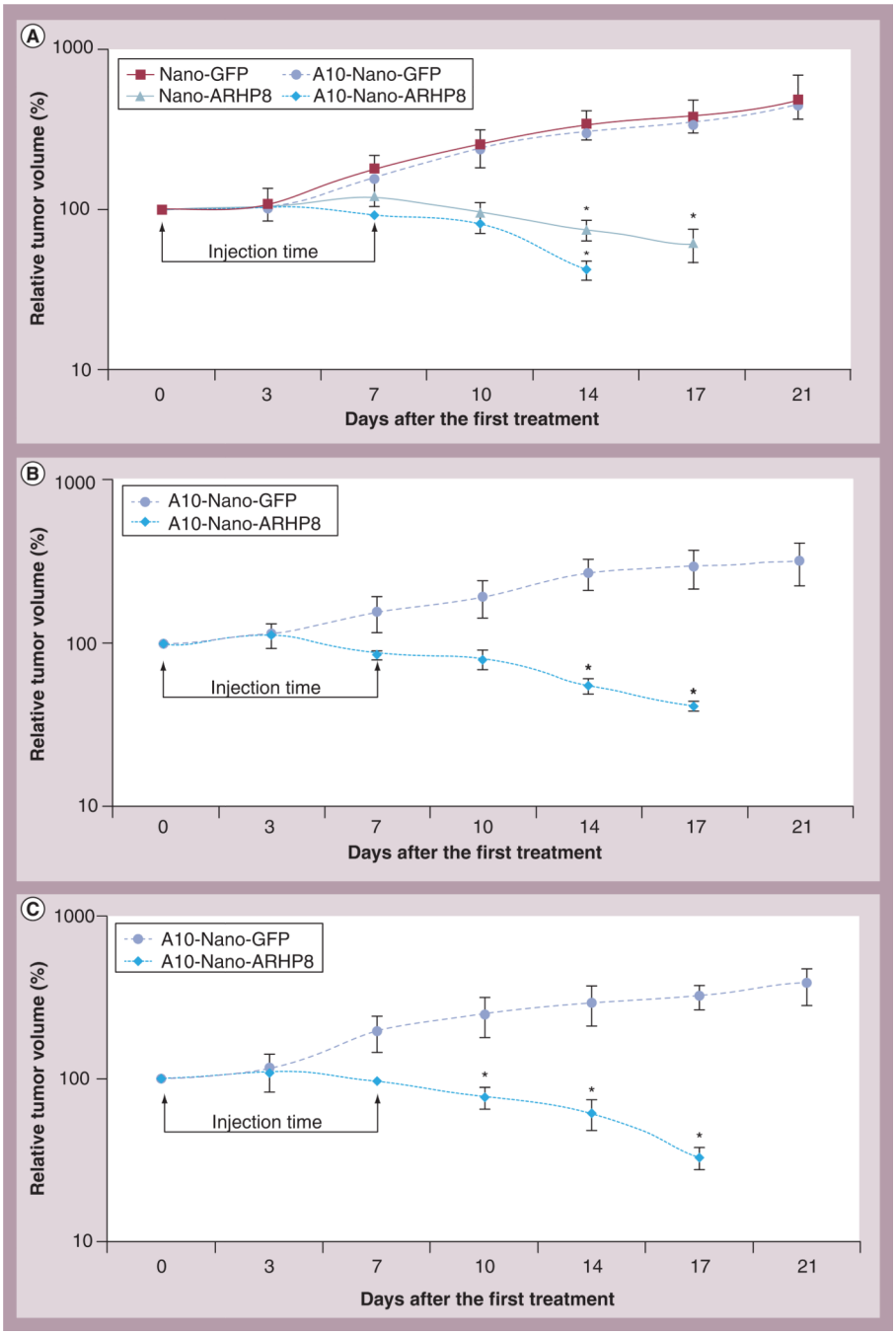

Figure 1. ARHP8 nanoparticles induce xenograft tumor eradication in nude mice

(A) Xenograft tumors were established in nude mice with 22RV1, **(B)** LAPC-4 or **(C)** LNCaP cells. Once tumors were palpable (~30–50 mm^3 in volume), animals were divided into different groups to receive various nanoparticles (n = 8). Nanoparticles were injected via tail vein in a volume of 200 μl that contains 4.0 μg plasmid DNA. A second dose was delivered in 1 week. Animals were monitored for tumor growth for 3 weeks. Data shows the average value of relative tumor volume (%) at the measuring time-point compared with the initial size at the first nanoparticle injection. Error bars represent the standard error of the mean. The vertical axis is in log scale.

*Significant difference compared with the control ($p < 0.05$, Student's *t*-test).
GFP: Green fluorescent protein.

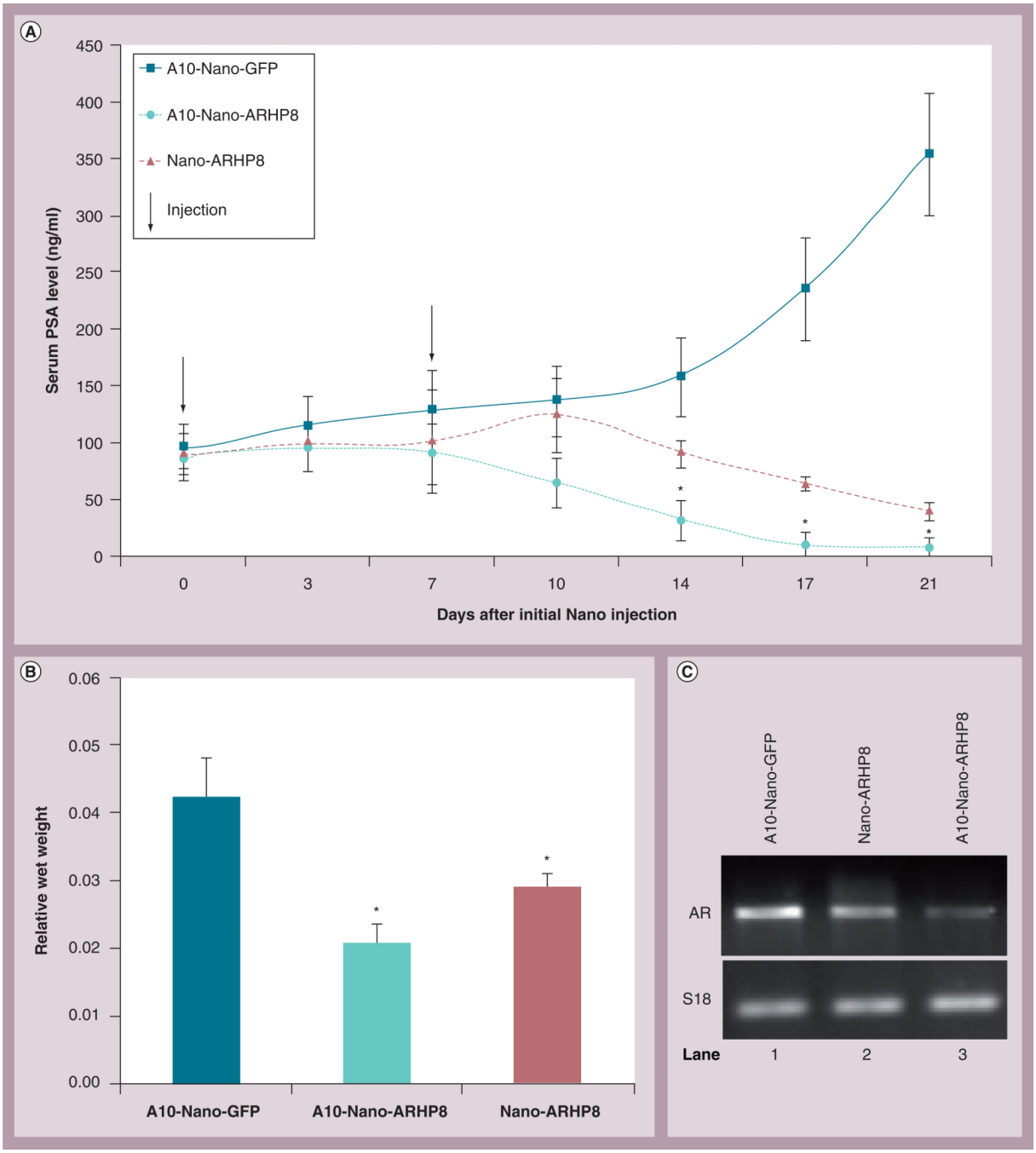

Figure 2. ARHP8 nanoparticles reduces serum prostate-specific antigen levels in nude mice

Orthotopic xenograft tumors were established in nude mice with LNCaP cells by inoculating 2×10^5 cells in 10 μl volume of culture media. Blood samples were collected through tail incision and serum PSA levels were monitored every week. Once serum PSA levels reached 70–90 ng/ml, animals were divided into three groups (n = 8) to receive different nanoparticles. Nanoparticles were injected via tail vein in a volume of 200 μl that contains 4.0 μg plasmid DNA. A second dose was delivered in 1 week. Animals were monitored for PSA levels for another 3 weeks. **(A)** Data shows the average value of serum PSA and the standard error of the mean. **(B)** Mouse prostate loops were harvested at sacrifice and the wet

weight was recorded. **(C)** Total RNAs were extracted from frozen tissue samples of the prostate loops and reverse transcription-PCR analysis was conducted to assess the *AR* gene expression.

*A significant difference compared with the control ($p < 0.05$, Student's *t*-test).

AR: Androgen receptor; GFP: Green fluorescent protein; PSA: Prostate-specific antigen.

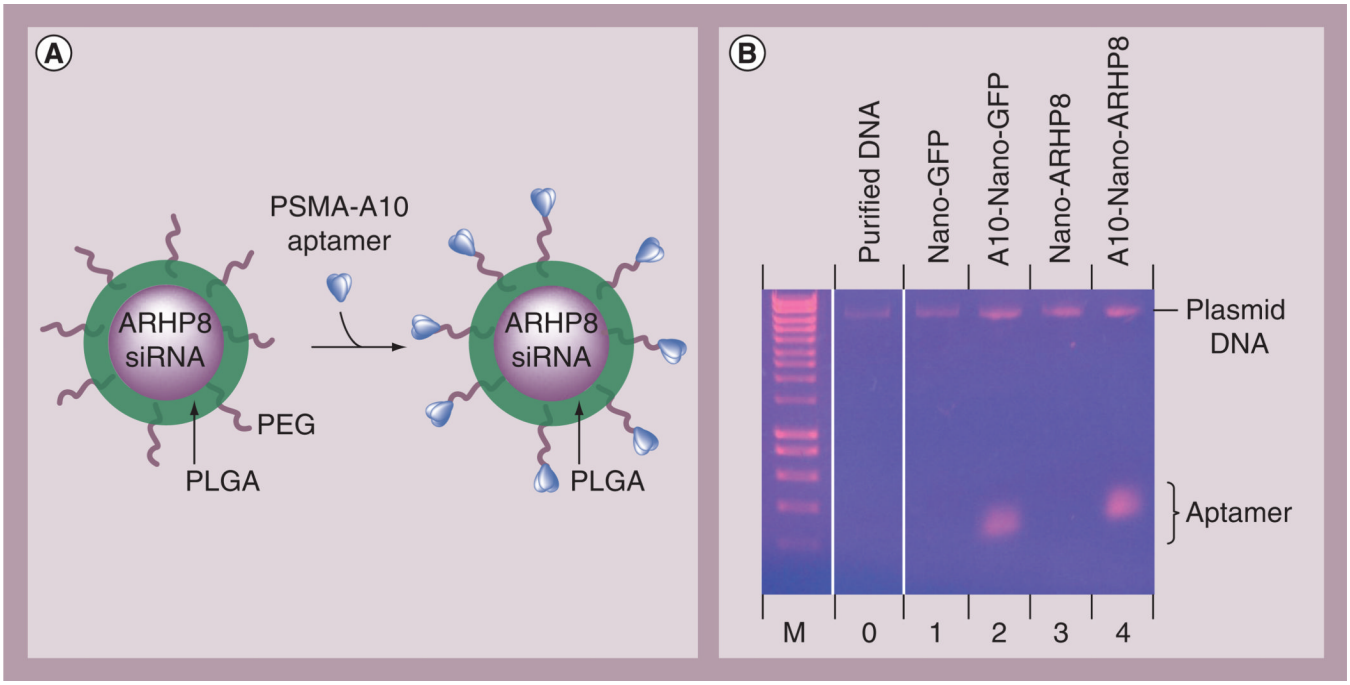

Figure 3. Nanoparticle-aptamer bioconjugation

(A) PLGA nanoparticles were modified by covalent conjugation with a PEG spacer. The RNA aptamer A10 that recognizes the human PSMA extracellular domain was conjugated onto the PEG spacer. **(B)** Confirmation of aptamer conjugation onto nanoparticles. Agarose gel image of plasmid DNA and A10 aptamer extracted from different nanoparticles.
GFP: Green fluorescent protein; M: Marker; PEG: Polyethylene glycol; PLGA: Poly-$_{DL}$-lactic-*co*-glycolic acid; PSMA: Prostate-specific membrane antigen.

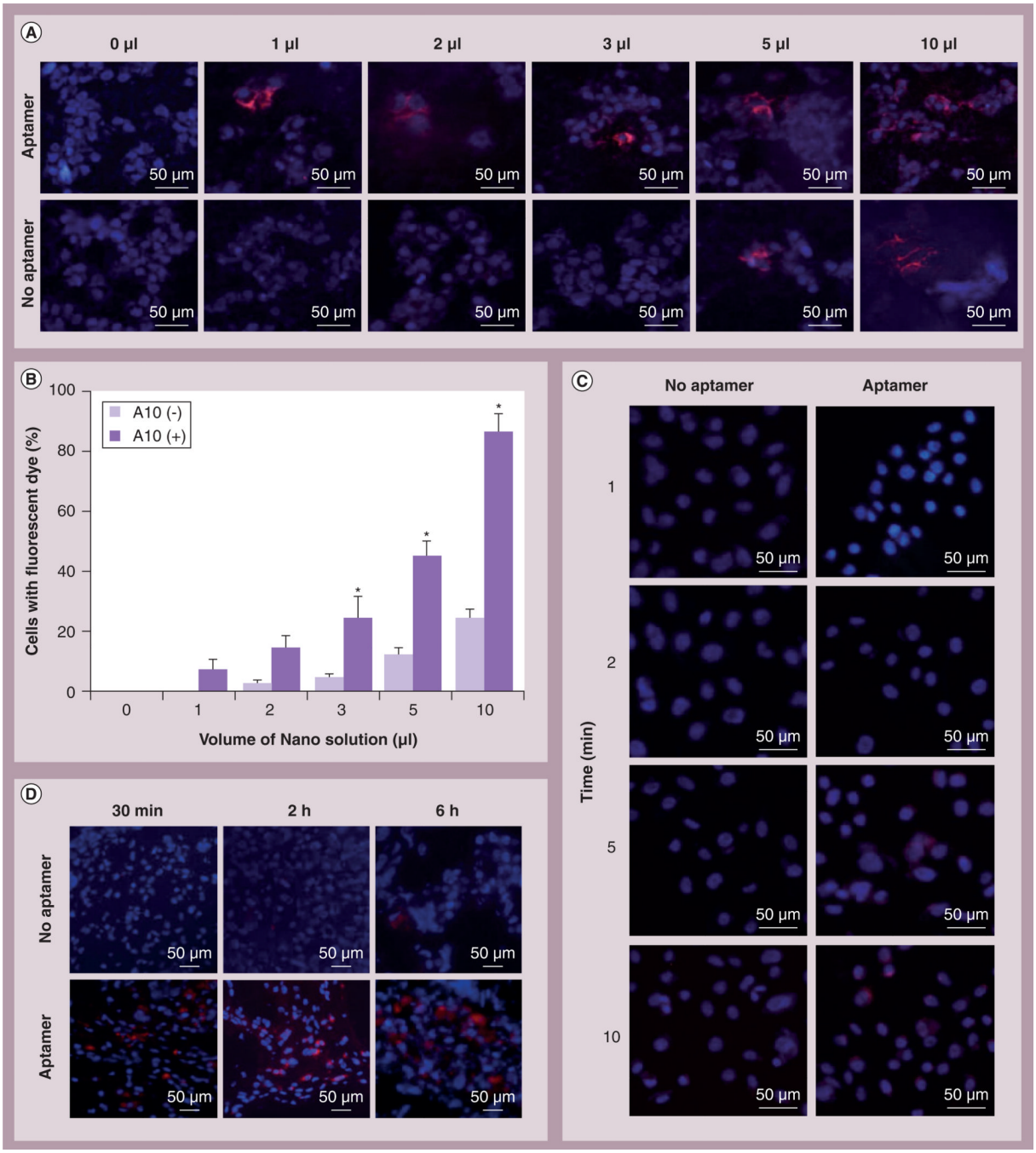

Figure 4. Cellular uptake of nanoparticles with or without A10 Aptamer

(A) Different amounts of nanoparticle loaded with Nile-red fluorescent dye were added to LNCaP cell culture media and 1 h later, cells were stained with blue nuclear dye Hoechst 33324. Quantitative data were summarized in panel **(B)** and error bars represent the standard error of the mean. **(C)** A total of 3 µl nanoparticles were added in cell culture for the indicated time period and the cell nuclei were visualized with Hoechst 33324 staining. **(D)** Tumor uptake of nanoparticles *in vivo*. 22RV1-derived xenografts were established in nude mice, and 150 µl nanoparticles were injected via tail vein. Xenografts were harvested at indicated time points after injection. Frozen sections were prepared and the cell nuclear

DNA was stained with 4',6-diamidino-2-phenylindole. Sections were evaluated under a fluorescent microscope.
Magnification ×200.
*Significant difference compared with the control ($p < 0.01$, student's *t*-test).

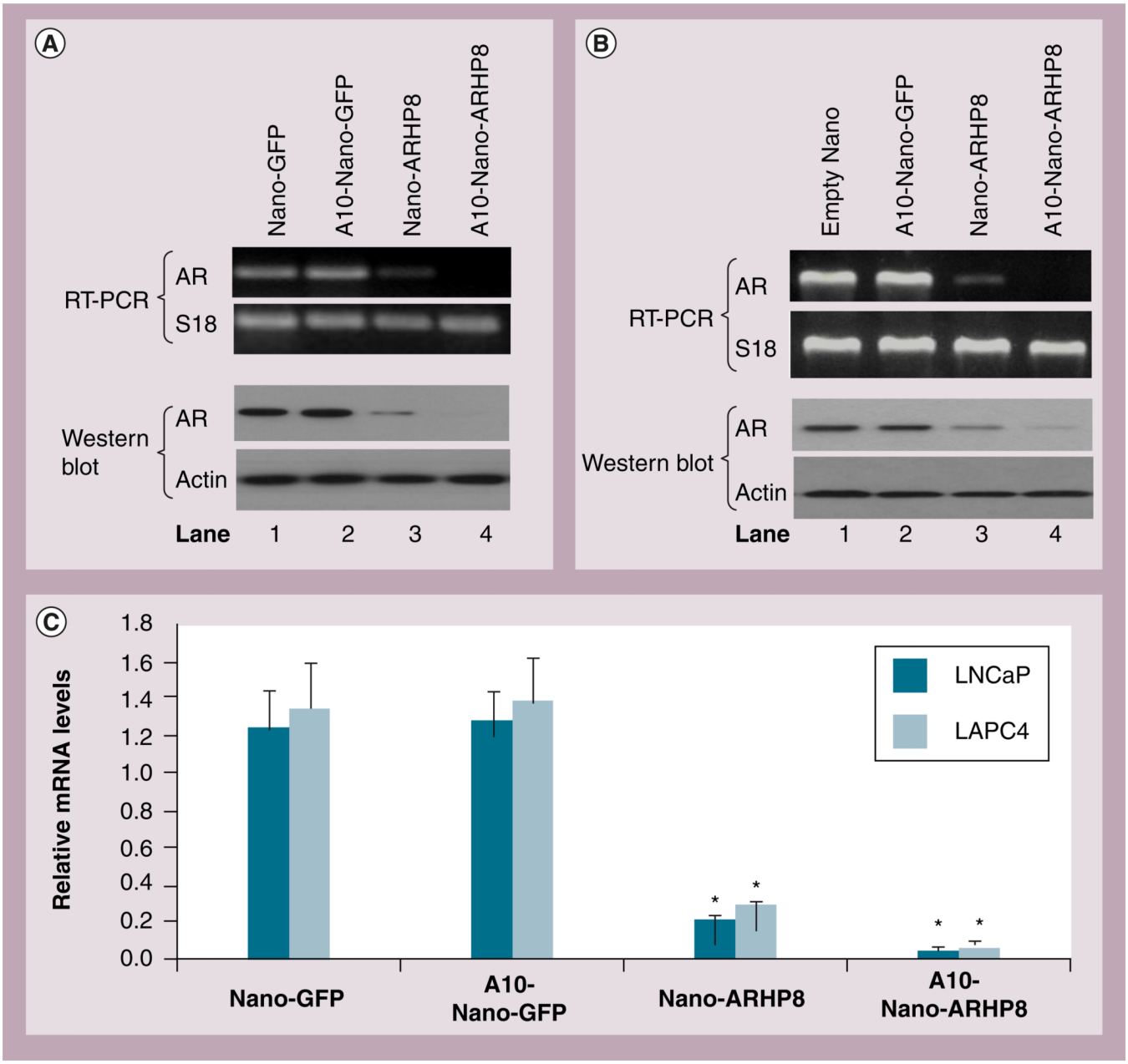

Figure 5. ARHP8-loaded nanoparticle-mediated *AR* gene silencing

(A) LNCaP or **(B)** LAPC-4 cells were placed in six-well plates overnight and then different nanoparticles were added into cell culture media at a dose of 2 μg DNA/well. Cells were harvested 7 days later and the total RNAs were extracted for RT-PCR and the *S18* gene was used as an internal control. Cell lysates were used in western blot assays and anti-Actin blot served as protein loading control. **(C)** Total RNAs from panel **(A)** and **(B)** were used for quantitative RT-PCR to assess *AR* gene expression. Error bars represents the standard error of the mean.

*Significant difference compared with the control ($p < 0.05$, Student's *t*-test).

AR: Androgen receptor; GFP: Green fluorescent protein; RT-PCR: Reverse transcription-PCR.

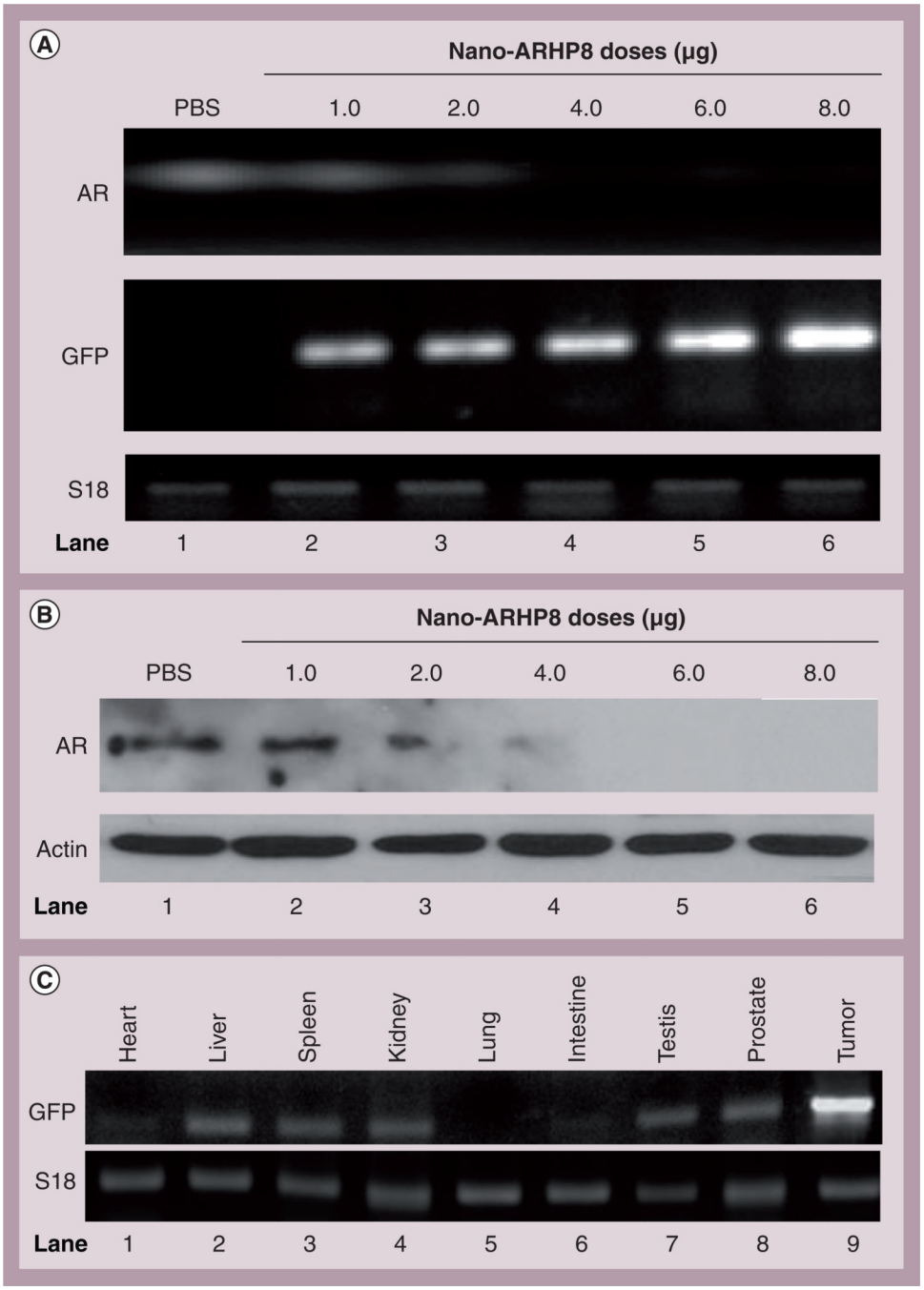

Figure 6. Pilot experiment for dose determination of ARHP8 nanoparticle-mediated *AR* gene silencing

Xenograft tumors were established in nude mice with human prostate cancer cells PC-3/AR. Once tumors were palpable (~30–50 mm^3 in volume), Nano-ARHP8 nanoparticles were injected via tail vein. A total of five different doses were used. One animal was injected with PBS as a negative control. After 1 week, animals were sacrificed and xenograft tumors, together with various major organs, were harvested for further analysis. **(A)** Total RNAs were extracted for reverse transcription-PCR analysis for AR mRNA and GFP mRNA expression. S18 was used as an internal control. **(B)** Protein extracts were prepared from xenograft tumors and probed with anti-AR antibody for AR protein levels. Actin blot served

as a loading control. **(C)** Genomic DNA extracts from xenograft tumor and major organs of the animal were used as templates in the PCR reaction to detect GFP sequence on the ARHP8 shRNA vector for the purpose of nanoparticle distribution.
AR: Androgen receptor; GFP: Green fluorescent protein; PBS: Phosphate-buffered saline.

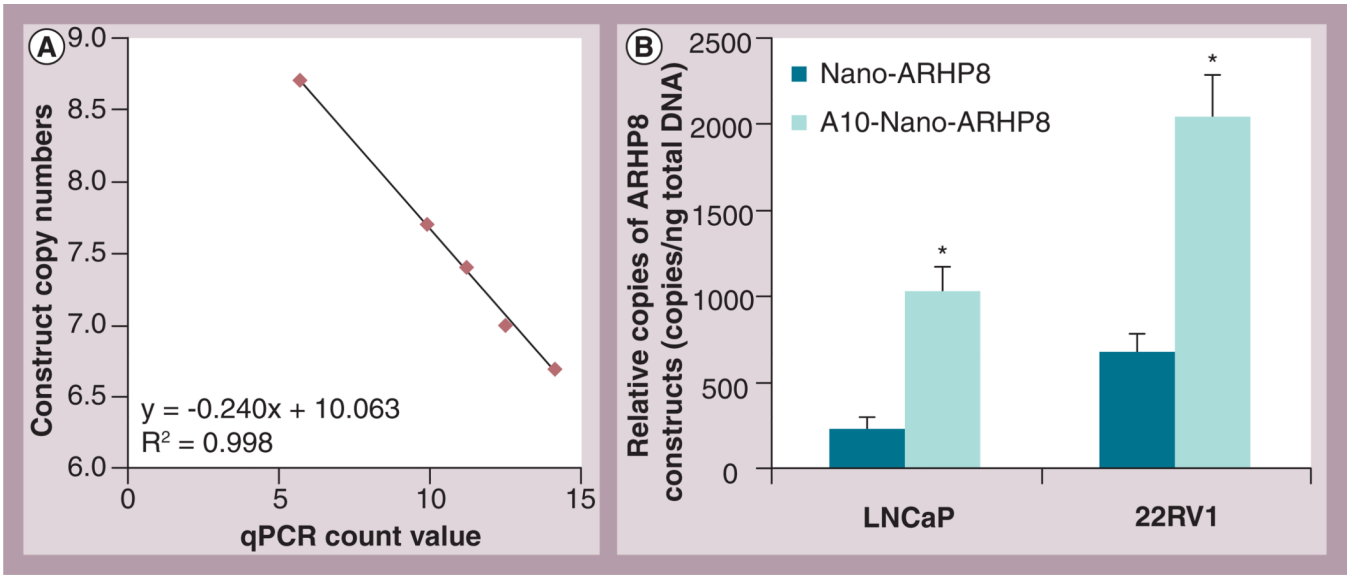

Figure 7. Prostate-specific membrane antigen A10 conjugation increases nanoparticle retention in prostate cancer xenografts

(A) The qPCR standard curve was generated using a serially diluted ARHP8-GFP construct as a template. **(B)** Genomic DNA samples were extracted from xenograft ssmples derived from 22RV1 and LNCaP cells as described in Figure 1 and used for quantitative PCR analysis of GFP expression. The relative construct copy numbers in the tissue were calculated based on the molecular weight of the ARHP8-GFP plasmid construct.

*A significant difference in A10-Nano-ARHP8 groups compared with the nonconjugated Nano-ARHP8 group ($n = 4$, $p < 0.05$, Student's *t*-test).

GFP: Green fluorescent protein; qPCR: Quantitative PCR.

Table 1

Characteristics of poly-DL-lactic-*co*-glycolic acid nanoparticles.

Nanoparticles	Nano-GFP	A10-Nano-GFP	Nano-ARHP8	A10-Nano-ARHP8
Size ± SD (nm)	244 ± 1.9	244 ± 4.1	185 ± 0.5	185 ± 0.1
Polydispersity	0.27 ± 0.01	0.26 ± 0.01	0.11 ± 0.04	0.17 ± 0.01
Zeta potential ± SD (mV)	−16.1 ± 1.95	−16.3 ± 0.91	−25.4 ± 0.66	−24.8 ± 0.52
Plasmid DNA loading (μg/ml)	20	20	21	21
Encapsulation efficiency (%)	93.1 ± 1.5	84.1 ± 1.4	72.6 ± 1.8	73.5 ± 1.8
Total surface area (m^2/g PLGA)	18.4	18.4	24.2	24.2
Surface aptamer (pMol/cm^2)	N/A	5.8	N/A	4.6

[a]GFP: Green fluorescent protein; N/A: Not applicable; PLGA: Poly-DL-lactic-co-glycolic acid; SD: Standard deviation.